Epitaxial growth of ZnO films on Si(111)

Ashutosh Tiwari,[a] M. Park, C. Jin, H. Wang, D. Kumar, and J. Narayan
Department of Materials Science and Engineering, North Carolina State University, Raleigh, North Carolina 27695-7916

(Received 20 May 2002; accepted 23 July 2002)

In this paper, we report the growth of ZnO films on silicon substrates using a pulsed laser deposition technique. These films were deposited on Si(111) directly as well as by using thin buffer layers of AlN and GaN. All the films were found to have *c*-axis-preferred orientation aligned with normal to the substrate. Films with AlN and GaN buffer layers were epitaxial with preferred in-plane orientation, while those directly grown on Si(111) were found to have random in-plane orientation. A decrease in the frequency of the $E_2^{(2)}$ Raman mode and a red shift of the band-edge photoluminescence peak due to the presence of tensile strain in the film, was observed. Various possible sources for the observed biaxial strain are discussed.

During the last few years wide-band-gap semiconductors have attracted significant scientific and technological interest.[1–3] ZnO holds a special position in materials physics due to its interesting electrical and optical characteristics.[1,2] Because of its higher exciton binding energy (60 meV) and higher luminescent efficiencies it is considered a substitute for GaN of the III–V semiconductor family[3] for various optical and light emitting applications. Its band gap (3.28 eV) is quite close to that of GaN (3.44 eV). The band gap of GaN can be increased or decreased by alloying with AlN (6.2 eV) or with InN (1.9 eV). Similarly, ZnO can be alloyed with MgO (8.2 eV) to increase the band gap or with CdO (2.0 eV) to decrease it.

For the use of ZnO in light emitting and nonlinear optical applications, high-quality single-crystal ZnO films are required. Epitaxial films of ZnO have been previously grown on (0001) planes of sapphire by the domain epitaxy mechanism.[4,5] The growth of high-quality ZnO films on silicon is expected to offer additional advantages as it will provide opportunity to integrate various functional properties of ZnO with the advanced silicon-based microelectronics devices. However, direct growth of epitaxial ZnO films on silicon is extremely difficult; often it results in inferior quality films.[6] Here, we report the epitaxial growth of ZnO films by employing buffer layers of AlN and GaN in a pulsed laser deposition process. This is the first report of growth of epitaxial ZnO on Si(111) with an AlN buffer layer; however, epitaxial growth of ZnO on Si(111)/GaN has been reported earlier.[7] We have also deposited ZnO directly on hydrogen-terminated Si(111) surfaces.

One of the most crucial factors that affect the performance of thin-film devices is the presence of biaxial strain (and associated stress) in the films.[8,9] It has been realized that the band structure of ZnO may change with the strain and subsequently may modify the optical and electrical characteristics of the film. We have investigated the strain present in these films as reflected on photoluminescence and Raman scattering measurements. The shift in the value of photoluminescence band-edge energy and the position of the $E_2^{(2)}$ Raman active phonon mode is used to characterize the sign and the relative magnitude of the stress present in these films.

Thin-film deposition was performed in a multitarget laser deposition chamber with a KrF excimer laser (Lambda Physik 210, $\lambda = 248$ nm). Energy density and repetition rate of the laser beam were 2–3 J/cm^2 and 10 Hz, respectively. Before deposition, Si(111) substrates were treated with 5% hydrofluoric acid solution to remove the surface oxide layer. AlN and GaN films were deposited in the vacuum (1×10^{-7} torr) at 700 °C, while ZnO films were deposited at 650 °C in an ambient oxygen pressure of 1×10^{-5} torr. The thickness of the AlN and GaN layers was approximately 100 nm, and that of the ZnO layer was approximately 500 nm. The thickness of individual layers was precalibrated against the number of pulses. X-ray diffraction (XRD) measurements were performed using Cu K_α radiation and a nickel filter. Selected area electron diffraction patterns were obtained by cross-sectional transmission electron microscopy (TEM) using a JEOL-2010F analytical microscope. Micro Raman spectroscopy measurements were carried out at

[a]Address all correspondence to this author.
e-mail: atiwari@unity.ncsu.edu

room temperature in the backscattering geometry with the 514.5-nm (2.41 eV) line of an Ar ion laser using an ISA U-1000 scanning double monochromator (JOBIN YVON, USA). Laser power of 120–140 mW was used to excite the sample. It was ensured that the excitation laser beam did not cause any heating of the sample. Photoluminescence (PL) measurements were performed using a Hitachi F-4500 FL spectrophotometer.

Figure 1 shows the XRD pattern of ZnO films grown on Si(111). In all the three cases we could obtain only the peaks corresponding to the (0002) planes of ZnO, AlN, GaN, the (111) peak of the Si, and the (0004) peak of ZnO. This indicates that all the films have *c*-axis-preferred orientation. However, the XRD reveals the alignment of the films only in the direction normal to the film. To determine the in-plane alignment of these films, we performed TEM investigations on various parts of these films. We found that while the films grown on Si(111) with AlN and GaN buffer layers are epitaxial, those grown directly on Si(111) show random in-plane orientation. In Fig. 2 we show the selected area diffraction pattern from ZnO film in the Si(111)/AlN/ZnO heterostructure. Well-aligned spots clearly establish the epitaxial nature of ZnO films. Figure 2(b) shows the diffraction pattern from the ZnO/AlN interface. Comparing this with standard diffraction patterns we found that ZnO and AlN have the following orientational relationship: ZnO[2$\bar{1}\bar{1}$0]||AlN[2$\bar{1}\bar{1}$0] along the in-plane direction and ZnO[0001]||AlN[0001] along the normal to the plane. ZnO and GaN layers in the Si(111)/GaN/ZnO heterostructure were found to have similar orientational relationships.

Figure 3(a) shows the Raman spectra of ZnO films deposited on various substrates. Raman spectra of Si(111) substrate and single-crystal ZnO are also shown for comparison. Since the ZnO, GaN, and AlN films are transparent in the 514-nm excitation, the intense Raman peak (520 cm^{-1}) from Si substrate was observed in all the three samples. The Raman spectra indicate that the ZnO films have a wurtzite structure. The wurtzite form of ZnO belongs to the C_{6v}^4 ($P6_3mc$) space group. According to the group theoretical analysis, the following optical modes exist at the Γ point of the Brillouin zone of the ZnO:

$$\Gamma = A_1(TO,LO) + 2B_1 + E_1(TO,LO) + 2E_2 \quad .$$

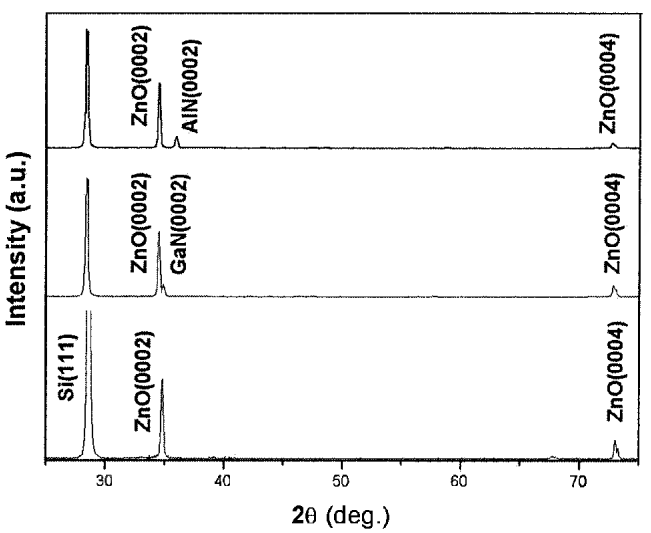

FIG. 1. X-ray diffraction patterns of Si(111)/AlN/ZnO, Si(111)/GaN/ZnO, and Si(111)/ZnO.

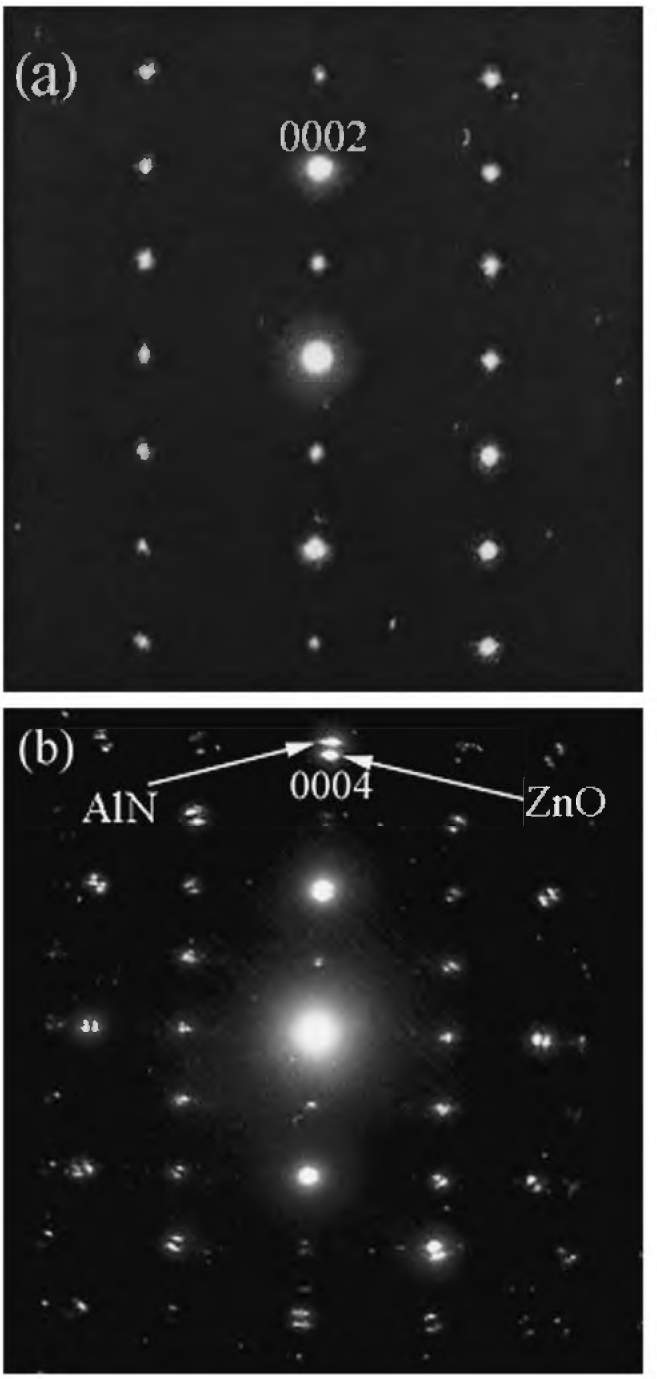

FIG. 2. Selected area diffraction pattern from cross section TEM sample of ZnO/AlN/Si (a) ZnO film only (b) ZnO/AlN interface.

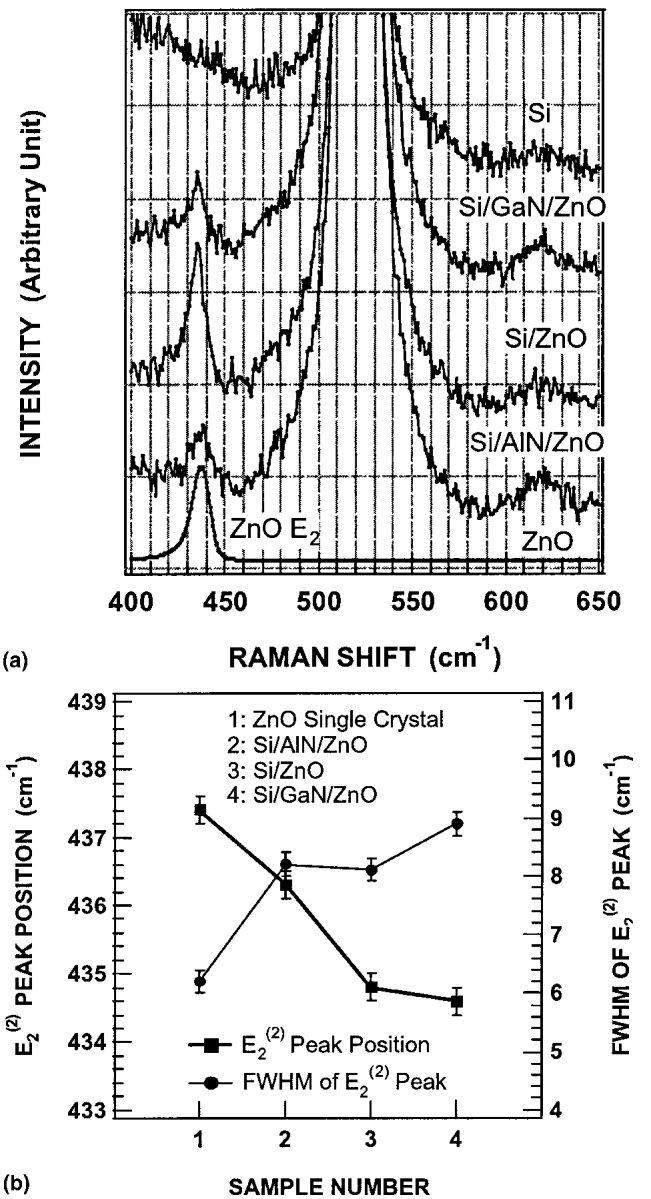

FIG. 3. (a) Raman spectra of various ZnO films. Raman spectra of Si(111) substrate and single-crystal ZnO are also shown for comparison. (b) Position and FWHM of Raman $E_2^{(2)}$ peaks for various ZnO samples.

Among these optic modes, two B_1 modes are silent, and A_1, E_1, and E_2 modes are Raman active. The A_1 and E_1 modes further split into transverse and longitudinal component due to their polar nature. The A_1 and E_1 modes are polarized along and perpendicular to the *c* axis of the hexagonal unit cell of ZnO, respectively. The E_2 modes have a low- and high-frequency submode, which are commonly designated as $E_2^{(1)}$ and $E_2^{(2)}$ modes, respectively. It has been observed that the position of the $E_2^{(2)}$ peaks is sensitive to any kind of pressure or stress in the film.[10]

Our analysis showed that the peak at around 437 cm^{-1} corresponds to the $E_2^{(2)}$ mode of ZnO. We fitted it with a Lorentzian function using a linear background. The position and full width at half-maximum (FWHM) of the Raman $E_2^{(2)}$ peaks are shown in Fig. 3(b). As is evident from this figure, the $E_2^{(2)}$ peak shifts to the lower frequency side as the substrate is changed from AlN/Si to Si and GaN/Si. The peak position obtained from the single-crystal ZnO was used as the reference point. A decrease in the frequency shift of the $E_2^{(2)}$ mode suggests the presence of tensile stress (and associated strain) in these films. By comparing our results with those of Mitra *et al.*,[11] we made an estimate that few kbars of tensile stress exist in our films. The FWHM of $E_2^{(2)}$ peak depends on the quality of the sample. As can be seen in Fig. 3(b), the FWHM of $E_2^{(2)}$ peaks for our films is about 30–50% higher than that for ZnO single crystal. This indicates that the crystal quality of bulk single crystal is much higher than that of films.

In Fig. 4 we show the room-temperature PL spectra of the ZnO films. For comparison, we have also shown the room-temperature PL spectrum of single-crystal ZnO. Because of the large exciton binding energy, 60 meV, excitonic emission survives even above room temperature. The band-edge maximum PL intensity peak for self-standing stress-free single-crystal ZnO films and bulk has been reported[12] to occur at about 3.285 eV. The PL peaks of the films in our study occur at slightly lower energies. This red shift in the PL peak is in agreement with the tensile strain as observed in Raman spectrum. At lower energies we observed a very broad PL peak. This broad peak has been observed previously also by several workers and is usually referred as the green band.[13] Reynolds *et al.*[13] attributed the origin of the green band to

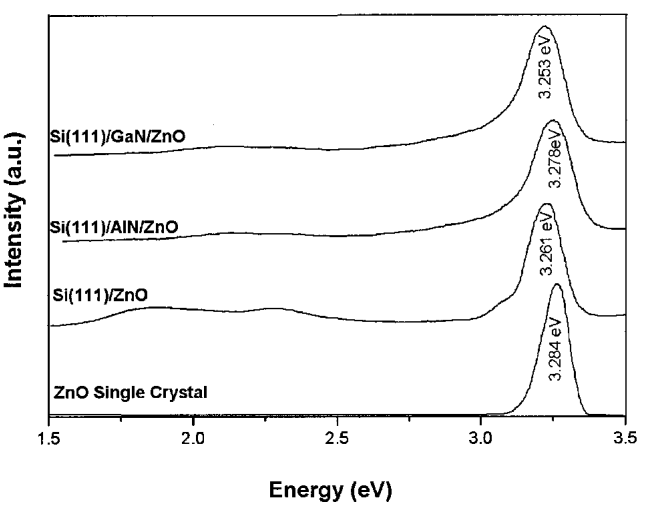

FIG. 4. Room-temperature PL spectrum of various ZnO films. For comparison, we have also shown the room-temperature PL spectrum of single-crystal ZnO.

defect states in the material. These defect states could be due to the presence of oxygen vacancies in the film. The intensity of the green band is greatest for the Si(111)/ZnO; this shows that the films directly grown on Si(111) have a greater number of defects and/or oxygen vacancies.

Strain in thin-film systems usually has the following three origins: (i) the lattice mismatch between the film and substrate (or buffer layer); (ii) difference in the thermal expansion coefficient of the film and substrate (or buffer layer); (iii) microstructure/defect related internal stresses. The lattice mismatch arises due to the differences in lattice constants between the film and the substrate under epitaxial growth conditions. If the lattice constant of the film a_f is less than the lattice parameter of substrate ($a_f < a_s$), then there is a tensile stress in the film; on the other hand, if ($a_f > a_s$), then the film is under compressive strain. Under the lattice matching, total strain is given by $\epsilon_T = 2(a_f - a_s)$. Since the in-plane lattice parameter of ZnO is more than that of AlN and GaN (see Table I), lattice mismatch strain in ZnO is expected to be compressive in the case of Si(111)/AlN/ZnO and Si(111)/GaN/ZnO heterostructures. The film directly grown on Si(111) has random in-plane orientation, and hence lattice mismatch strain is expected to be absent in this film. Furthermore, it has been reported that beyond a critical thickness of the film most of the lattice mismatch stress gets dissipated in creating dislocations in the film at the growth temperature. However, as the film cools down, the thermal strain is developed in the film due to the difference in the thermal expansion coefficient of the substrate and the film. If the coefficient of thermal expansion of the films α_f is greater than the coefficient of thermal expansion of the substrate α_s ($\alpha_f > \alpha_s$), then the thermal strain in the film is expected to be tensile; on the other hand, if $\alpha_f < \alpha_s$, then the thermal strain will be compressive in nature. As can be seen in Table I, the value of the coefficient of thermal expansion of ZnO along the *a–b* basal plane is less than those of AlN, GaN, and Si; this implies that the thermal strain in ZnO film should be compressive. The third cause of the strain, namely, the microstructure/defect related internal stress, is resulting from the trapped point defects like vacancies, interstitials, dislocations, etc. If vacancies with lower specific volume compared to the host lattice are present, then a net tensile stress prevails in the film. Oxygen vacancies in ZnO films are expected to cause tensile strain. Since the net strain in the ZnO films, as determined by a decrease in the frequency of $E_2^{(2)}$ mode of Raman spectra and a red-shift of the band-edge PL peak, is tensile, we predict that the microstructure/defect related internal stress is the main source of the strain in the system.

TABLE I. Lattice parameters and the coefficients of thermal expansion of Si, AlN, GaN, and ZnO along the *a–b* basal plane.

	Lattice parameter (Å)	Thermal expansion coefficient (K^{-1})
Si	$a = 5.431$	3.6×10^{-6}
AlN	$a = 3.112$; $c = 5.186$	4.5×10^{-6}
GaN	$a = 3.189$; $c = 5.185$	5.6×10^{-6}
ZnO	$a = 3.252$; $c = 5.213$	2.9×10^{-6}

In conclusion, we have grown and integrated single-crystal epitaxial ZnO films on Si(111) substrates by employing AlN and GaN buffer layers in a pulsed laser deposition process. A thorough investigation of their optical characteristics has been carried out using Raman scattering and PL experiments. Growth of epitaxial ZnO films on silicon substrates with a precise understanding of their optical characteristics provides excellent opportunity to integrate various functional properties of ZnO with the silicon-based microelectronics devices.

ACKNOWLEDGMENTS

This work was partially supported by the National Science Foundation. The authors thank Prof. R.J. Nemanich for very useful comments and permission to use the micro-Raman facilities.

REFERENCES

1. H. Ohno, Science **281,** 951, 1998.
2. Z.K. Tang, P. Yu, G.K.L. Wong, M. Kawasaki, A. Ohtomo, H. Koinuma, and Y. Segawa, Solid State Commun. **103,** 459 (1997).
3. H. Morkoç, S. Strite, G.B. Gao, M.E. Lin, B. Sverdloy, and M. Burns, J. Appl. Phys. **76,** 1363 (1994).
4. A. Tiwari, C. Jin, A. Kvit, D. Kumar, J.F. Muth, and J. Narayan, Solid State Commun. **121,** 371 (2002).
5. G.J. Exarhos and S.K. Sharma, Thin Solid Films **270,** 27 (1995).
6. T. Shirasawa, T. Honda, F. Koyama, and K. Iga, in *III-V Nitrides,* edited by F.A. Ponce, T.D. Moustakas, J. Akasaki, and B.A. Monemar (Mater. Res. Soc. Symp. Proc. **449,** Warrendale, PA, 1997), p. 373.
7. A. Nahhas, H.K. Kim, and J. Blachere, Appl. Phys. Lett. **78,** 1511, 2001.
8. B.H. Bairamov, O. Gürdal, A. Botchkarev, H. Morkoç, G. Irmer, and J. Monecke, Phys. Rev. B **60,** 16741 (1999).
9. A. Konkar, A. Madhukar, and P. Chen, Appl. Phys. Lett. **72,** 220 (1998).
10. F. Decremps, J. Pellicer-Porres, A.M. Saitta, J-C. Chervin, and A. Polian, Phys. Rev. B **65,** 92101 (2002).
11. S.S. Mitra, O. Brafman, W.B. Daniels, and R.K. Crawford, Phys. Rev. B **186,** 942 (1969).
12. F. Decremps, J. Pellicer-Porres, A.M. Saitta, J-C. Chervin, and A. Polian, Phys. Rev. B **65,** 92101 (2002).
13. D.C. Reynolds, D.C. Look, B. Jogai, and H. Morkoç, Solid State Commun. **101**(9), 643 (1997).